OPEN ACCESS
IOP Publishing
Nanotechnology

Nanotechnology **36** (2025) 152501 (25pp)
https://doi.org/10.1088/1361-6528/adb635

Perspective

Perspective: magnetic quantum sensors for biomedical applications

Kai Wu* and **Rui He**

Department of Electrical and Computer Engineering, Texas Tech University, Lubbock, TX 79409, United States of America
E-mail: kai.wu@ttu.edu
and *rui.he@ttu.edu*

Abstract
With advancements in thin-film deposition, nanofabrication, and material characterization techniques, quantum devices leveraging nanoscale quantum phenomena have emerged across various fields, including quantum computing, sensing, communication, and metrology. Among these, quantum sensing harnesses the unique properties of quantum systems to achieve highly sensitive and precise measurements of physical quantities such as magnetic and electric fields, temperature, pressure, and even biological events. In this perspective, we highlight some popular magnetic quantum sensors used for magnetic sensing and imaging, and emerging spintronic quantum sensors that exploit the quantum mechanical properties of electron spin for similar applications. Most of the techniques discussed remain in lab-based stages, with limited preliminary data reported. However, the authors believe that, with continued progress in spintronics, these nano- and micro-scale spintronic devices—offering superior and unique magnetic quantum properties—could open new horizons in biomedical applications, including single-cell and single-molecule detection, large-scale protein profiling, sub-micrometer resolution medical imaging, and beyond.

Keywords: quantum sensor, spintronics, magnetic sensor, magnetic imaging, biomedical application

1. Introduction

In December 2023, the US National Institutes of Health (NIH) announced 'Notice of Special Interest (NOSI): Quantum Sensing Technologies in Biomedical Applications' [1], expressing a special research interest that advances quantum sensing toward biomedical applications. Quantum sensors rely on quantum phenomena to detect subtle changes in the physical properties of their surrounding environment. Operating at the nanoscale, these sensors exploit principles such as superposition, entanglement, and tunneling, enabling them to achieve exceptional precision in detecting minute environmental changes. They can potentially realize single molecules or single cells detection for bioassays and nanometer-scale resolution for medical imaging, revolutionizing the next generation of healthcare. To date, different types of quantum sensors that are based on different quantum principles have been tailored for different biomedical applications [2, 3]. A variety of quantum sensors have been researched, and some have even reached clinical stages. For medical imaging, examples of quantum

* Author to whom any correspondence should be addressed.

sensors include magnetic resonance imaging (MRI), superconducting quantum interference device (SQUID), positron emission tomography (PET), single photon emission CT (SPECT), etc. For high-sensitivity bioassays, examples of quantum sensors include chip-based magnetoresistive (MR) biosensors, chip-based nuclear magnetic resonance (NMR) biosensors, portable nanodiamonds containing nitrogen-vacancy (NV) biosensors, quantum dots (QDs), etc.

In this perspective, we focus on the emerging class of magnetic quantum sensors for biomedical applications. In section 2, we categorize different sensor types based on their usage and further classify magnetic biosensors based on the target signal, such as label-based and label-free approaches, followed by an introduction to magnetic quantum sensors. In section 3, we highlight some common types of magnetic quantum sensors, including SQUIDs, MRI, optically pumped magnetometers (OPMs), NV magnetometers, and QDs. Some of these magnetic quantum sensors are already employed in clinical applications. For instance, in neuroimaging, SQUIDs are used in magnetoencephalography (MEG) to enable highly sensitive detection of weak magnetic fields generated by neuronal activity, facilitating real-time brain imaging with high spatial and temporal resolution. This technology enhances our understanding of brain function and assists in diagnosing and monitoring neurological disorders. In cardiac imaging, SQUIDs are used in magnetocardiography (MCG) to map the magnetic fields produced by the heart's electrical activity, aiding in the diagnosis of cardiac conditions by providing detailed heart rhythm and abnormality imaging. In section 4, we provide an outlook on spintronic devices, which are emerging quantum sensors for magnetic sensing. These range from mature devices like MR sensors to lab-stage devices such as spin-torque oscillators (STOs), spin-Hall oscillators (SHOs), 2D van der Waals (vdW) magnets, and skyrmions. We analyze the current development status of these spintronic devices as next-generation magnetic quantum sensors and discuss the steps needed to bring them into clinical use.

2. Targeted biomedical applications

2.1. Different types of sensors according to usage

Sensors have a broad range of applications in the biomedical field, significantly impacting diagnostics, treatment, and patient monitoring. Wearable sensors are non-invasive devices worn externally, such as on the skin, wrist, or clothing, to monitor physiological parameters like heart rate and activity. The sports bracelet products in the market are an example of wearable sensors. They provide real-time data, are easy to use, and are particularly suited for continuous monitoring in everyday settings, making them ideal for managing chronic conditions and enhancing health monitoring without disrupting the user's daily life. Implantable sensors, in contrast, are invasive devices surgically placed inside the body to provide long-term, *in vivo* monitoring of internal conditions. Glucose sensors and pacemakers are representative examples. Implantable sensors offer high precision and are better suited for applications requiring localized measurements or continuous data from internal organs. Portable sensors, also known as point-of-care devices, provide rapid, on-site testing for infectious diseases, metabolic disorders, cancers, etc. Their portability makes them especially valuable in remote or underserved areas where access to centralized healthcare facilities is limited. Bulky system sensors, typically found in hospitals and clinics, are designed for advanced diagnostics, monitoring, and treatment. These systems often incorporate highly sensitive and precise sensors integrated into sophisticated medical equipment, such as MRI and CT scanners. They can capture detailed physiological and anatomical data, making them indispensable for diagnosing complex conditions and guiding treatment decisions. Unlike

portable or wearable sensors, these systems require specialized environments, including controlled settings (e.g. cryogenic, magnetic shielding, etc) and trained personnel, to operate effectively. Their bulkiness often results from the need for high-resolution imaging, powerful data processing capabilities, and robust hardware for long-term reliability. While they offer unparalleled accuracy and comprehensive insights, their size and operational complexity limit their use in clinical settings.

2.2. Magnetic sensors for biomedical applications

In the area of biological sensors, i.e. biosensors, sensors can be categorized based on the target signal they are designed to detect: (1) electrochemical biosensors (e.g. glucose sensors, cholesterol sensors), (2) optical biosensors (e.g. surface plasmon resonance sensors, fluorescence-based sensors), and (3) magnetic biosensors (e.g. MRI scanner, MR biosensors). Because biological entities and tissues are typically diamagnetic or paramagnetic, they generate negligible magnetic signals compared to the strong signals produced by magnetic tags or biological events-caused magnetic fields. Magnetic tags, commonly made of iron oxide nano-/micro-particles, offer several advantages, including high biocompatibility, stability in harsh environments, and resistance to optical bleaching (unlike fluorescent tags). These properties make magnetic biosensors highly sensitive and robust, making them ideal for various biomedical applications [4].

Magnetic biosensing can be categorized into two approaches based on the detection mechanism: label-based and label-free. The label-based approach is commonly used for detecting non-magnetic biomarkers (e.g. proteins, nucleic acids, and cells) in disease diagnosis. In this method, biomarkers are specifically labeled with magnetic tags, enabling quantitative sensing. The binding events (e.g. antibody–antigen, DNA–DNA, DNA–protein interactions) cause the magnetic tags to produce detectable magnetic signals to the magnetic biosensor, providing a readable signal that indicates the quantitative results.

Label-free magnetic sensing detects targets directly without the need for magnetic tags, by measuring changes in the magnetic properties or signals associated with the target. Medical imaging techniques, such as MEG, MCG, and magnetomyography (MMG), are examples of label-free magnetic sensing. MEG detects the magnetic fields generated by neuronal activity, typically ranging from picotesla (pT) to nanotesla (nT), with frequencies spanning 0.5–100 Hz. These signals enable real-time studies of brain activity. MCG measures the magnetic fields produced by cardiac activity throughout the cardiac cycle. Although cardiac magnetic fields (10–100 pT) are stronger than those generated by neurons, they remain weak compared to the Earth's magnetic field ($\sim$50 μT). These fields, with frequencies from 0.5 Hz to 20 Hz, reflect key components of the cardiac cycle, such as the P-wave (atrial depolarization), QRS complex (ventricular depolarization), and T-wave (ventricular repolarization). MMG measures the magnetic fields generated by the electrical activity of muscles during contraction, resulting from ionic currents associated with action potentials traveling along muscle fibers. These fields typically range from femtotesla (fT) to pT, with frequencies between 5 Hz and 300 Hz.

2.3. Magnetic quantum sensors

Magnetic quantum sensors are advanced devices that utilize quantum mechanical principles to achieve ultra-sensitive detection of magnetic fields and magnetic tag-labeled biomarkers. These sensors are particularly promising in biomedical imaging due to their ability to detect ultra-low bio-magnetic fields with high

spatial and temporal resolution. However, there is a significant gap in translating these quantum sensors for practical biomedical applications.

For example, to enable *in vitro* magnetic biosensing, magnetic quantum sensors must undergo surface chemical modification to functionalize them for specific binding of biomarkers. This involves coating the sensor surface with biocompatible and functional molecules, such as antibodies, peptides, or aptamers, which selectively bind to target proteins, nucleic acids, or pathogens. Surface modification methods are crucial to transforming the sensors into functional biosensors while maintaining their quantum properties and sensitivity. In section 4.1, we will showcase some successful examples of transforming MR sensors into functionalized biosensors for *in vitro* bioassay applications.

For wearable applications, additional engineering adaptations are critical to addressing the inherent limitations of magnetic quantum sensors. Some existing sensors, such as SQUIDs and MRI systems, are unsuitable for wearable use in non-magnetically shielded environments. SQUIDs rely on cryogenic cooling and require highly shielded environments to achieve their ultra-high sensitivity, making them bulky and impractical for integration into wearable platforms. Similarly, MRI systems depend on large superconducting magnets, which are neither portable nor adaptable to wearable formats. In contrast, quantum sensors like OPMs [5, 6] offer greater potential for wearable applications due to their ability to operate at room temperature and in environments with less stringent magnetic shielding. Despite this advantage, these sensors still demand significant engineering improvements to enable compatibility with flexible, biocompatible substrates that can conform to the human body while ensuring stable and reliable performance. Emerging spintronic magnetic quantum sensors, such as MR sensors, are also being actively explored for fully flexible, wireless, and compact designs that enable real-time MCG and MEG measurements [7, 8]. Addressing key challenges like reducing power consumption, mitigating electromagnetic interference, and improving signal processing algorithms is essential for advancing these wearable sensors.

Although less commonly seen in quantum sensors, if used in implantable applications, additional considerations are necessary to ensure that sensors function reliably within the complex biochemical and mechanical environment of the human body. These quantum sensors must be designed to operate stably over extended periods while being biocompatible and minimally invasive. Flexible and miniaturized designs are critical for conforming to tissue surfaces or embedding within specific organ structures, such as the brain or heart, without causing significant discomfort or damage [9, 10]. Furthermore, low power consumption and wireless data transmission capabilities are essential to reduce heat generation and the need for invasive wires, enhancing the practicality of these quantum devices for long-term implantation.

For both *in vitro* and *in vivo* applications, an appropriate sensor encapsulation step is required to isolate these quantum sensors from the biological environment [11, 12]. This encapsulation serves several purposes: (1) it protects the sensors from corrosion or degradation caused by exposure to biological fluids, (2) it prevents potential adverse interactions, such as immune responses or tissue inflammation, (3) it ensures mechanical stability by safeguarding the sensor from stresses induced by bodily movements or tissue interactions, and (4) it provides a platform for functionalizing the sensor surface with biorecognition elements, enabling selective binding of biomarkers for biosensing applications. Common encapsulation materials, such as polyimide, parylene C, and ultrathin oxide films, can achieve these objectives while maintaining the sensitivity of the sensor to target signals.

Lastly, the integration of a robust signal recording and filtering system is crucial for ensuring accurate data collection and the successful application of

magnetic quantum sensors in biomedical settings. In non-magnetically shielded environments, environmental noise can substantially impair sensor performance, necessitating advanced noise suppression techniques. Additionally, artifacts caused by mechanical movements of the subject, such as muscle contractions or shifts in sensor placement, can introduce random noise that affects the reliability of the measurements. To address these challenges, advanced signal processing techniques, including noise cancellation algorithms, adaptive filtering, and machine learning-based artifact removal, should be implemented. Additionally, the integration of reference sensors to measure and subtract environmental noise in real-time can further improve signal fidelity. These measures will be critical to ensuring that magnetic quantum sensors deliver reliable and clinically meaningful data for biomedical applications.

3. Current magnetic quantum sensors

3.1. SQUID

SQUID, a highly sensitive magnetic field sensor, consists of a superconducting loop interrupted by one (RF SQUID) or two (DC SQUID) Josephson junctions, as shown in figure 1(a) for a DC SQUID. A Josephson junction is a thin insulating layer between two superconducting materials that allows quantum tunneling of cooper pairs (pairs of electrons in a superconducting state). SQUID detects changes in magnetic flux by converting them into a measurable voltage, leveraging quantum interference within the superconducting loop to achieve remarkable sensitivity. The magnetic flux threading the loop is quantized, and an external magnetic field induces a screening current to maintain this quantization. This changes the phase difference across the junctions, modulating the supercurrent in the loop. When a bias current is applied, the voltage across the junctions oscillates periodically with the magnetic flux, with a period equal to the magnetic flux quantum. This enables precise detection of ultra-weak magnetic fields down to the fT/sqrt (Hz) range [13–15]. DC SQUIDs, with their superior sensitivity, are widely used in biomedical applications such as MCG and MEG [16]. In contrast, RF SQUIDs, with a single junction, are simpler but less sensitive and suitable for less demanding applications.

Despite their extraordinary sensitivity, SQUIDs have limitations. Their operation requires superconducting materials, which necessitate cryogenic conditions maintained by liquid helium or advanced cooling systems. This requirement imposes constraints on portability and increases the cost and complexity of the setup, making SQUIDs less practical for certain applications. To address this limitation, research is focused on developing high-temperature superconducting materials that can operate at more accessible temperatures, reducing the reliance on cryogenic cooling [20]. Additionally, advancements in miniaturization and integration of cooling systems may help reduce the complexity and cost of SQUID setups, improving their portability and practicality for a wider range of applications.

3.2. MRI

MRI is another non-invasive medical imaging modality that works on the principle of NMR [21]. Where hydrogen protons of water in the body are exposed to a strong static magnetic field, causing their macro-spins to align with the field. When an RF pulse is applied, these macro-spins are knocked out of alignment. As the protons' macro-spins relax back to their original alignment, the changes in the magnetic field are detected to form an image. The relaxation process occurs via two processes: T1 (longitudinal) and T2 (transverse). T1-weighted images highlight tissues with high-fat content, while T2-weighted images better visualize

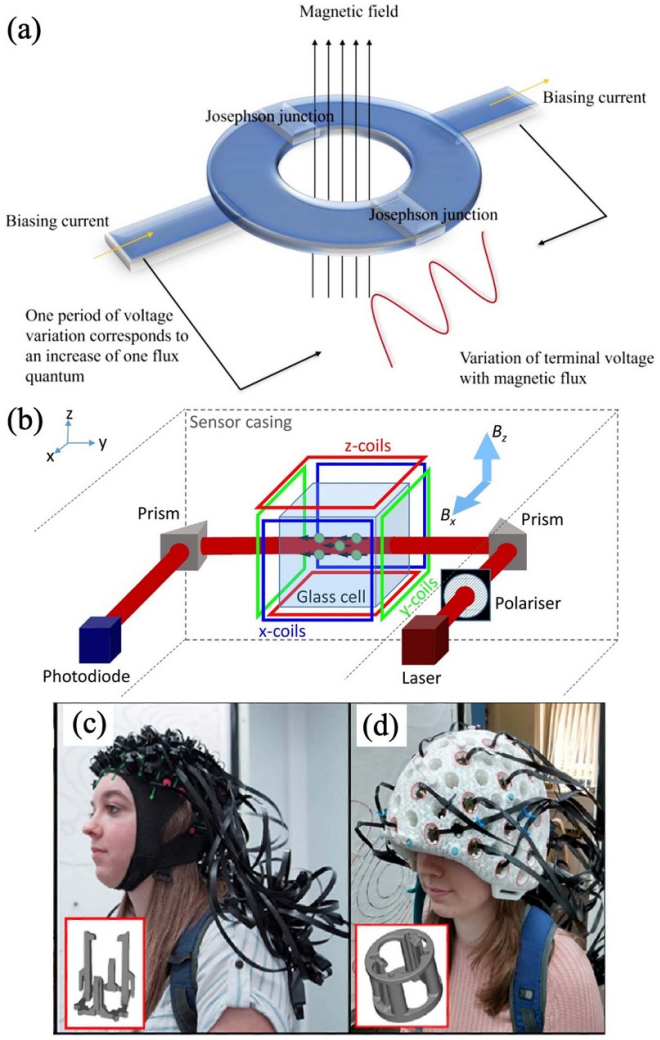

Figure 1. Working principles of (a) Josephson junctions in SQUID and (b) OPM. (a) Reproduced from [17]. CC BY 4.0. (b) Reproduced from [18]. CC BY 4.0. The (c) flexible cap and (d) rigid helmet OPM-MEG systems. Both helmets contain push-fit clips to house the 2nd generation QuSpin OPMs. Reproduced from [19]. CC BY 4.0.

fluid, like water, within tissues, allowing for differentiation between normal anatomy and abnormalities like inflammation or tumors based on their fluid content. Magnetic tags are often used as contrast enhancers in MRI to improve the imaging. Where these magnetic tags create localized magnetic field inhomogeneities that affect the relaxation times of surrounding water protons, leading to changes in signal intensity during MRI. This improves the contrast between different tissues, making it easier to detect abnormalities such as tumors or inflammation. MRI and contrast-enhanced MRI have been extensively studied regarding working principles and clinical applications [22, 23], this Perspective will not elaborate on this.

While MRI is a powerful non-invasive medical imaging modality, it faces several technical challenges for its widespread use. One of the key challenges is the need for strong static magnetic fields, typically generated by superconducting magnets, which require cryogenic cooling. This imposes significant operational costs and limits the portability and accessibility of MRI systems. Researchers are exploring the development of high-temperature superconducting materials that can operate at more manageable temperatures, thus reducing the reliance on cryogenic cooling and lowering costs. Another challenge is the limited spatial

resolution at lower magnetic field strengths, which can hinder the detection of small-scale abnormalities. Higher field strengths, such as 3 T or more, provide better resolution but increase the cost and cooling requirements. In response, advancements in magnet design and the development of more efficient superconducting magnets are being pursued to improve both resolution and cost-effectiveness [24, 25]. Additionally, MRI systems are highly sensitive to magnetic field inhomogeneities, which can reduce image quality, especially in regions with high susceptibility to artifacts. This can be addressed by employing advanced magnetic field shimming techniques [26, 27] to ensure a more homogeneous magnetic field, thereby improving image quality. Lastly, the need for magnetic contrast agents, to enhance imaging further introduces complexity and risks related to biocompatibility. Continued research on biocompatible, targeted magnetic nanoparticles is crucial for overcoming these hurdles and improving the effectiveness of MRI in clinical practice.

3.3. OPM

OPM measures magnetic fields by exploiting the quantum properties of polarized atomic spins, typically in alkali or noble gases. As shown in figure 1(b), in OPM, a laser tuned to a specific wavelength (resonant with the atomic transition) optically pumps the atoms into a specific quantum state, and their interaction with an external magnetic field causes spin precession at the Larmor frequency, which is proportional to the magnetic field strength. This precession modifies the polarization of a second probe beam passing through the gas, which is then used to measure the Larmor frequency and magnetic field strength. OPMs are compact, operate at room temperature, and achieve exceptional sensitivity, detecting magnetic fields as weak as ∼fT/sqrt(Hz) [28–30]. They are used in biomedical applications such as MCG, MEG, and MMG [5]. Miniaturized OPMs have also been reported [29, 31]. Commercial products of OPM for MEG are already available at suppliers such as Brainbox Ltd.

Numerous clinical applications of OPMs for wearable MEG recording have been demonstrated in recent years [18, 19, 32–34]. For instance, Hill *et al* developed two wearable OPM mounting methods for MEG recording: a flexible cap (figures 1(c)) and a rigid helmet (figure 1(d)) [19]. While both designs enable high-quality data acquisition, the authors highlight the rigid helmet as the more robust option, offering significant advantages for reconstructing field data into 3D images of neuronal current changes. Through repeated measurements in two participants, they demonstrated the device's reliability in signal detection. Additionally, using source-space modeling, the study revealed that, despite utilizing five times fewer sensors, their OPM-MEG system achieves performance comparable to a traditional cryogenic SQUID-MEG device.

A major issue of OPM is the sensitivity to environmental noise, which can compromise their accuracy. This necessitates the use of magnetically shielded environments, which adds cost and limits portability. To address this, active noise cancellation and advanced signal processing algorithms are being developed to improve signal extraction in noisy environments [35, 36]. Additionally, the performance of OPMs can be affected by temperature fluctuations, which impact the stability of the atomic gas and the laser system. Thermal stabilization techniques can mitigate these effects. When integrating OPMs with biological systems for applications like MEG, MCG, and MMG, where motion artifacts from the subject can degrade measurements. The development of wearable OPMs [6, 37] with motion correction algorithms is a promising solution. Furthermore, miniaturizing OPMs while maintaining their sensitivity requires advancements in microfabrication techniques and compact optical components. Continued research and engineering innovations are critical to overcoming these challenges and unlocking the full potential of OPMs in biomedical applications.

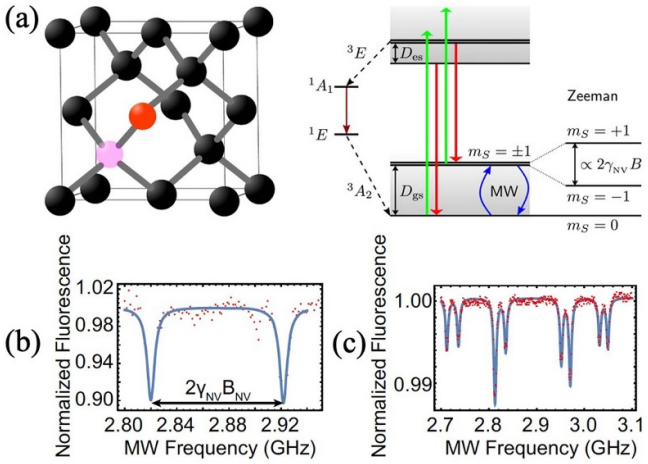

Figure 2. (a) Working principles of NV magnetometer. Reproduced with permission from [38]. © 2021 The Authors. Advanced Quantum Technologies published by Wiley-VCH GmbH. CC BY-NC-ND 4.0 (b) ODMR spectrum of a single NV center, enabling the determination of the magnetic field along the NV axis. (c) ODMR spectrum of an ensemble of NV centers with the magnetic field applied along an arbitrary direction, revealing four distinct B-field projections on different NV axes. By analyzing such spectra, the full B-field vector can be reconstructed. Reproduced from [39], with permission from Springer Nature.

3.4. NV magnetometers

NV magnetometers operate based on the unique quantum properties of NV centers, atomic-scale defects in diamonds consisting of a nitrogen atom adjacent to a lattice vacancy. These centers have electronic spin states ($|m_s = 0\rangle$ and $|m_s = \pm 1\rangle$) that are highly sensitive to magnetic fields. As shown in figure 2(a), the NV center is optically initialized into the $|m_s = 0\rangle$ state using a 532 nm laser, and fluorescence intensity is used to read out the spin state. When exposed to a magnetic field, the $|m_s = \pm 1\rangle$ states undergo Zeeman splitting, where the energy levels shift in proportion to the magnetic field strength (see figure 2(b)). By applying microwave radiation near the NV center's resonance frequency induces transitions between the $|m_s = 0\rangle$ and $|m_s = \pm 1\rangle$ states, with the resonance frequency depending on the local magnetic field. Using optically detected magnetic resonance (ODMR) spectroscopy, the magnetic field strength is determined by monitoring fluorescence changes as the microwave frequency is varied, enabling nanoscale imaging (see figures 2(b) and (c)). For NV magnetometers, it is crucial that when conducting measurements in the presence of a magnetic field greater than a few mT, the field is aligned with the axis of the NV centers. This alignment is essential because transverse magnetic fields can cause quenching of the NV fluorescence and a loss of ODMR contrast, which would compromise the accuracy of the measurements.

Single NV centers typically achieve sensitivities around $\sim\mu$T/sqrt(Hz), and ensembles of NV centers can enhance sensitivity to $\sim$pT/sqrt(Hz) due to the collective signal averaging effect [40]. This exceptional sensitivity, combined with room-temperature operation and nanoscale spatial resolution, makes NV magnetometers ideal for biomedical applications such as neuronal activity imaging, molecular-level imaging, and other precision magnetic field measurements. In addition, the NV magnetometers are robust and can function in a wide range of temperatures, from cryogenic up to hundreds of degrees Celsius (limited by the stability of the diamond and electronic components). Portable NV magnetometers are also reported by some labs [38, 41] and are commercially available by suppliers such as Qnami. In addition to magnetic field sensing, NV centers in diamonds are used for a variety of applications due to their sensitivity

to different physical properties. They can detect electric fields [42, 43], measure temperature [44, 45], and function as high-resolution sensors for biochemical interactions [46, 47]. NV centers also serve as qubits in quantum computing [48, 49].

While NV magnetometers offer exceptional properties, their application in biomedical sensing and imaging faces several technical challenges. One significant limitation is the requirement for precise alignment between the NV center's axis and the magnetic field, as misalignment can reduce sensitivity and accuracy [50, 51]. Solutions to this issue involve improving system designs to allow for easier alignment and employing advanced calibration techniques. Additionally, in biological environments, the presence of noise from surrounding magnetic fields and the need for efficient signal extraction in complex, heterogeneous samples can further complicate measurements. Techniques such as shielding, noise reduction, and advanced signal processing can be implemented to mitigate the noise issue. Furthermore, to facilitate integration with biological systems, innovations in sample preparation, as well as better control of environmental conditions, are needed to maintain both the stability of the NV centers and the biological specimens. Implementing these solutions will help maximize the potential of NV magnetometers for practical biomedical applications.

3.5. QDs

QDs are nanoscale semiconductor particles that exhibit unique optical and electronic properties due to the phenomenon of 'quantum confinement'. They are excellent fluorophores in biosensing due to their extraordinary optical properties. By surface functionalizing QDs with biomolecules (e.g. antibodies, aptamers, or peptides), they can selectively bind to proteins, DNA, or pathogens. When excited by light, QDs emit fluorescence, with the wavelength determined by their size and composition. This allows multiplexed detection of multiple targets in a single assay, enabling highly sensitive and specific disease diagnostics.

QDs are often combined with magnetic nanoparticles in biosensors to label and detect targets. This dual functionality—fluorescence for imaging and magnetic properties for separation—is particularly valuable in biomedical applications [52]. The fluorescent signal and magnetic signal of hybrid magnetic QDs are also exploited for multi-modal imaging [53]. The role of QDs in sensors is not limited to simple fluorescent tags for bioassays, it also extends to intrinsic sensors that utilize the inherent photophysical response of QDs to fluctuations in temperature, magnetic/electric fields, or ion concentration [54]. For example, graphene QDs (GQDs) can function as intrinsic magnetic field sensors by exploiting their spin-dependent optical properties and the Zeeman effect, which shifts their energy levels in response to an external magnetic field. These shifts can alter the photoluminescence spectra, making GQDs capable of detecting magnetic fields at the nanoscale. Recently, Ge *et al* reported giant orbital magnetic moments and the paramagnetic energy shifts linked to the interaction between magnetic fields and GQDs [55]. Although their work does not explicitly develop QDs as magnetic field sensors, it provides the foundational understanding of their magnetic behavior, supporting their potential application as magnetometers. Future research could build on these findings to design QD-based magnetometers for detecting weak bio-magnetic fields for medical imaging.

When it comes to practical biomedical applications, the potential toxicity, often due to heavy metals like cadmium, limits the clinical use of QDs. This is being addressed by developing non-toxic alternatives such as graphene QDs and silicon QDs [56, 57]. Stability in biological environments is another issue, as QDs can degrade or aggregate, affecting their fluorescence. Surface coatings like polyethylene glycol (PEG) improve stability and biocompatibility [58]. Target

Table 1. Comparison of different magnetic quantum sensors for biomedical applications.

	Sensitivity	Cost	Cryogenic	System	Current applications
SQUID	fT/sqrt(Hz)	High	Yes	Bulky	Medical imaging (Commercial)
MRI	—	High	Yes	Bulky	Medical imaging (Commercial)
NMR	—	Low	No	Portable	Bioassays (Commercial)
OPM	fT/sqrt(Hz)	Low	No	Portable	Medical imaging (Commercial)
NV magneto-meter	pT/sqrt(Hz)	Low	No	Portable	Magnetic sensing (Lab stage)
QD-based Magnetometer	NA	Low	No	Nanoparticle	Magnetic sensing (Lab stage)

specificity also depends on robust functionalization methods, with advances in click chemistry enhancing binding precision. Photobleaching reduces signal reliability but can be mitigated by core-shell structures or alloyed QDs.

Table 1 summarizes the sensitivity, cost, and operating conditions of current magnetic quantum sensors. Researchers are actively developing room-temperature quantum sensors to reduce operational costs and complexity, particularly for biomedical applications. While cryogenic conditions are essential for some types of quantum sensors, many others are designed to operate in ambient or near-ambient environments, broadening their applicability.

4. Emerging spintronic magnetic quantum sensors

Since the first report of the tunnel magnetoresistance (TMR) effect in 1975 [59] and the giant magnetoresistance (GMR) effect in 1988 [60, 61]. Spintronic devices, which leverage the intrinsic spin property of electrons, have experienced rapid growth over the past two decades. Spintronics uses the quantum mechanical property of electron spin (i.e. ‘up’ or ‘down’ states) and its associated electron charge. This dual functionality can lead to spintronic devices for high-speed unconventional computing, low power consumption data processing/storage, high data storage density, and great sensing performance [62–64]. The ongoing discoveries of new spintronic phenomena such as spin-transfer torque (STT), spin hall effect (SHE), spin-orbit torque (SOT), Rashba effect, Dzyaloshinskii–Moriya interaction (DMI), spin Seebeck effect (SSE), chiral-induced spin selectivity (CISS), etc., have unveiled more unique applications. In this section, we comment on some promising spintronic devices as quantum sensors for biomedical applications, specifically, magnetic sensing and imaging.

4.1. MR sensors

MR sensors are used to detect magnetic fields by monitoring changes in devices’ electrical resistances. They are widely used due to their high sensitivity, compact size, and versatility. They are essential in various fields, including data storage, biosensing, and navigation. Currently, there are three primary types of MR sensors: anisotropic magnetoresistance (AMR), GMR, and magnetic tunnel junctions (MTJs).

4.1.1. AMR sensors. AMR is a phenomenon where the electrical resistance of a ferromagnetic material changes depending on the angle between the current flow and the magnetization direction (figure 3(a)). This occurs because the scattering of conduction electrons varies with the relative orientation of their spin and the material’s magnetization, causing resistance to be higher when current flows parallel to the magnetization and lower when perpendicular (figure 3(e)). AMR sensors typically exhibit a small resistance change (2%–4%) and offer moderate

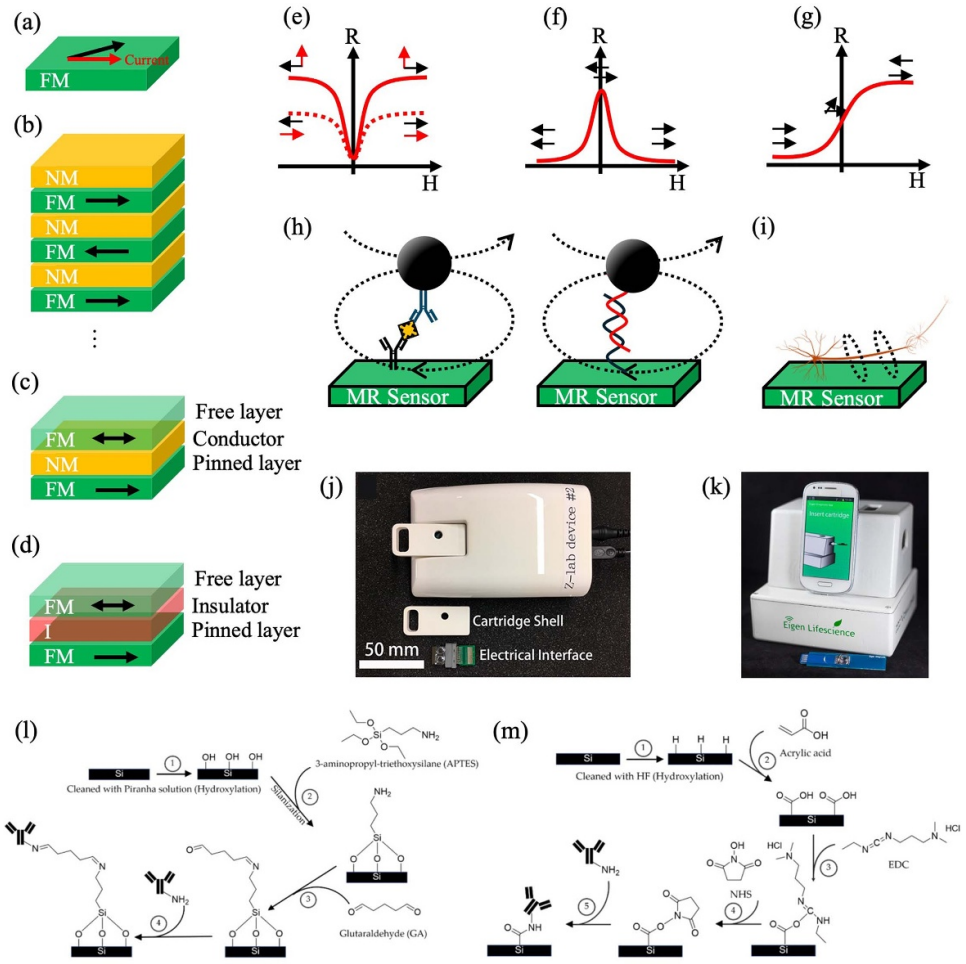

Figure 3. Schematics of (a) AMR, (b) GMR multilayer structure, (c) GMR SV, (d) MTJ. (e)–(g) Are the *R–H* curves of different MR sensors under varying external fields. Black and red arrows represent magnetization and current directions, respectively. (h) and (i) Illustrate MR sensors designed for label-based analyte detection and label-free detection of bio-magnetic fields associated with biological events, respectively. For simplicity, only the free layer, whose magnetization is influenced by local magnetic fields, is shown in the schematic. (j) and (k) Are photographs of reported GMR point-of-care devices. (j) Reprinted with permission from [66]. Copyright (2017) American Chemical Society. (k) Reprinted from [67], Copyright (2016), with permission from Elsevier. The procedures for the conventional (l) APTES-GA coating and (m) EDC/NHS coating. FM = ferromagnetic. NM = non-magnetic. I = insulator. Arrows represent magnetization directions in FM layers. Reproduced from [68]. CC BY 4.0.

field detection sensitivity (μT/sqrt(Hz)). They are commonly made from permalloy (NiFe alloy) and are used in applications such as compass sensors, current sensing, and linear position detection due to their simplicity and cost-effectiveness. Due to its moderate field detection sensitivity, AMR sensors are mainly used for industry and only very few reports of AMR sensors for biomedical applications [65].

4.1.2. GMR sensors. GMR multilayer sensors consist of alternating ferromagnetic and non-magnetic conductive layers (figure 3(b)). The resistance depends on the relative alignment of the magnetizations in adjacent ferromagnetic layers. When the magnetizations in adjacent layers align parallel, resistance is low; when they align antiparallel, resistance is high (figure 3(f)). GMR sensors show a significantly larger resistance change (10%–50%) compared to AMR and have high sensitivity to weak magnetic fields (nT/sqrt(Hz)) [69].

A variant of the GMR multilayer structure is the GMR spin-valve (GMR SV, figure 3(c)), which features fewer thin film stacks and improved sensing performance. In a GMR SV structure, one ferromagnetic layer, known as the free layer, is a soft magnetic material whose magnetization can be altered by an external magnetic field or magnetic tags on its surface. The other ferromagnetic layer, the pinned layer, is a hard magnetic material (or a soft magnetic material exchange coupled to a pinning layer) whose magnetization is fixed and requires a large field to switch. This pinned layer serves as a reference, allowing the relative magnetization directions of the two ferromagnetic layers to be measured. GMR SVs are designed so that the magnetizations of the free and pinned layers form a 90° configuration without an external field, producing an intermediate resistance. This configuration enables a linear resistance-field (R–H) response (figure 3(g)), making GMR SVs ideal for quantitative magnetic field measurements. As a result, a single GMR SV is optimized for detecting magnetic fields along a specific direction with high sensitivity.

One popular application of GMR sensors is for label-based biosensing. The first work of applying GMR sensors for biosensing was reported in 1998 by Baselt *et al*, where micrometer-sized Dynabeads were directly sensed by GMR sensors [70]. The authors forecasted that with further development of the GMR sensor technique, it is possible to be used for studying the single-molecule level interactions between DNA–DNA, antibody–antigen, ligand–receptor, etc. Over two decades of development, GMR sensors have been successfully applied for analyte detection of molecules, nucleic acids, viruses, cells, etc [12], combined with magnetic nanoparticles as labels (figure 3(h)).

GMR SV-based *in vitro* bioassays have been extensively explored in clinical settings for detecting a broad spectrum of diseases and pathogens, including SARS-CoV-2, Influenza A Virus (IAV), cirrhosis, Hepatitis B Virus (HBV), ovarian cancer, and more [66, 71–78]. Notably, GMR SV-based bioassays have also been integrated with nucleic acid amplification techniques such as polymerase chain reaction (PCR) and loop-mediated isothermal amplification (LAMP) to enable the detection of viral DNA or RNA, including human papillomavirus (HPV), HBV, complementary DNA (cDNA), and specific DNA mutations associated with cancer prognostics [79–81]. These advancements highlight the versatility of GMR SV-based biosensors in improving the sensitivity and specificity of molecular diagnostics for a wide array of clinical applications.

The label-free GMR sensing of bio-magnetic fields caused by biological events started in the 2010s (figure 3(i)). In 2011, Amaral *et al* reported the first use of GMR SV sensors to measure the magnetic field generated by action potentials in mouse brain slices [82]. Under stimulation near the CA3/CA1 border of the hippocampus, the GMR SV sensor recorded signals with an amplitude of 20 μV and a pulse length of 20–30 ms, which were detected exclusively in the pyramidal cell body region. The authors attributed this signal to the simultaneous stimulation of over 500 neurons. In 2017, Caruso *et al* placed five segments of 4×30 μm^2 GMR SV sensors on the tip of a needle to study the *in vivo* neural response in a cat's visual cortex [83]. The authors reported that event-related bio-magnetic fields in response to visual stimuli reached several nT, as detected by the GMR SV sensors. Although the signal-to-noise ratio (SNR) was still lower compared to electrophysiology, this proof of concept highlighted the potential of using spintronic devices for studying micro-scale physiological events.

4.1.3. MTJ sensors. MTJ sensors operate on the TMR effect, where electrons quantum-mechanically tunnel through an insulating barrier, such as MgO, sandwiched between two ferromagnetic layers, as shown in figure 3(d). The tunneling current—and hence resistance—varies depending on the relative alignment of the ferromagnetic layers' magnetizations. Parallel alignment allows

higher tunneling current and lower resistance, while antiparallel alignment results in lower current and higher resistance (figure 3(f)). MTJ sensors exhibit the highest resistance change (up to 600% or more) among all MR sensors and extreme sensitivity for magnetic field detection (pT/sqrt(Hz)) [84, 85].

Building on the success of label-based GMR biosensors for analyte detection, MTJ biosensors have recently emerged as a promising alternative, offering the potential for higher sensitivity. For instance, Sharma *et al* demonstrated the use of MTJ sensor arrays for detecting pathogenic DNA [86]. By integrating these sensors with microfluidic channels, they laid the groundwork for lab-on-a-chip systems, paving the way for advanced point-of-care diagnostic applications.

MTJ for label-free bio-magnetic field recording is also reported. In 2017, Sharma *et al* fabricated an array of 12 MTJ sensors, each with a junction area of $3 \times 40\ \mu m^2$, for the *in vitro* recording of the neuron signals from hippocampal slices [87]. MTJ sensors have also been demonstrated for cardiac signal recording. Fujiwara *et al* first reported the use of MTJ sensors for this purpose, achieving a minimum detectable magnetic field of 233 pT/sqrt(Hz) [88]. By incorporating a Wheatstone bridge design and applying signal averaging, they successfully measured the QRS complex from cardiac activity. Building on this, Wang *et al* developed an enhanced tri-axial MCG system using MTJ sensors [89]. Their results showed that the R-wave and QRS complex associated with the cardiac cycle were observable without the need for signal averaging. The amplitude of the R-peak recorded by the MTJ sensor in the *x*-direction was 200 pT, consistent with SQUID measurements after accounting for the distance between the observation point and the magnetic field source.

4.1.4. Preparing MR sensors for room temperature biomedical applications. To date, two start-up companies, Magic Lifescience Inc. and Zepto Life Technology Inc., were founded based on GMR biosensors, figures 3(j) and (k) show the photographs of GMR point-of-care devices. There are commercial products of MR sensors on the market, one example supplier is NVE corporation, most of these MR sensor products are packaged chips and used in industrial applications. The examples showcased above have shown that MR sensors hold significant potential for biomedical applications, but several challenges need to be addressed to fully realize their capabilities.

For quantitative magnetic sensing and imaging, the MR sensor's signal (R in R–H curves) must exhibit a unique correspondence with the magnetic field (H in R–H curves). Therefore, GMR SV and MTJ sensors with 90° magnetization configurations are preferred for magnetic sensing applications, as shown in figure 3(g). Additionally, the free layers of GMR SV and MTJ sensors (figures 3(c) and (d)) are designed to be sensitive only to external magnetic fields along a single axis. This design is sufficient for label-based magnetic biosensing, where magnetic tags can be intentionally magnetized by an applied field along the designated sensitive axis. However, for magnetic imaging, MR sensors require tri-axial sensitivities. This can be achieved by grouping three MR sensors, each measuring the magnetic field along a different axis. Such sensor groups can then be arranged into arrays for 2D imaging applications, including MCG, MEG, and MMG. The resolution of these arrays depends on the spacing between sensor groups and the magnetic field detectivity of individual sensors.

Theoretically, single-cell imaging resolution can be achieved by fabricating MR sensor arrays with inter-sensor gaps smaller than the size of a cell, a goal within reach using current nanofabrication techniques. However, existing GMR SV and MTJ sensors lack the sensitivity to detect the sub-fT to sub-pT magnetic fields generated by single-cell biological activity. For example, while the magnetic field produced by a single neuron firing ranges from 10 to 100 pT near the cell, cumulative neuronal activity generates only slightly stronger signals in

the nT range detectable at the scalp. For non-invasive magnetic imaging, the magnetic field strength generated by biological events decreases with the cube of the distance. Therefore, the distance between the MR sensor and the neurons or cells is a critical factor that puts a higher requirement on the sensor's sensitivity. Achieving the sensitivity required to detect such weak fields without cryogenic cooling remains a major challenge. To address this, methods such as integrating magnetic flux concentrators (MFCs), advanced signal post-processing, and signal averaging are being explored to enhance the SNR, potentially enabling reliable detection of weak bio-magnetic signals. Despite these advances, implementing these techniques in compact, portable devices remains a significant hurdle to overcome.

Biocompatibility is a significant challenge, particularly for implantable MR sensors used in critical tissues like the brain and heart. The potential risks associated with these applications include (1) electrical leakage from MR sensors and electrodes, (2) corrosion of MR sensors due to prolonged exposure to complex biochemical environments, and (3) biological contamination and tissue inflammation. To address these issues, MR sensors must be encapsulated with a thin layer of biocompatible materials such as polyimide, silicone, epoxy resin, or parylene C [90, 91]. However, encapsulation introduces another technical challenge: the increased distance between the biomagnetic field sources (e.g. neuron cells) and the sensors. Because magnetic field strength decreases with the cube of the distance, this added separation can significantly reduce the sensor's ability to accurately detect and map magnetic fields. Consequently, researchers must strike a balance between the thickness of the encapsulation layer and the sensor's detectivity. This trade-off is crucial to ensure adequate isolation of MR sensors from the biological environment while minimizing any adverse effects of increased sensor-to-source distance on sensing performance.

For *in vitro*, label-based magnetic bioassays using MR sensors, a critical step is surface modification to transform MR sensors into functional biosensors capable of detecting specific biological targets. To date, various surface modification techniques have been developed for rigid substrates such as glass, silicon, and polystyrene [92–96]. Among these, two widely adopted methods for MR sensor functionalization are (1) the 3-aminopropyltriethoxy silane/glutaraldehyde (APTES/GA, figure 3(l)) method [96] and (2) the 1-ethyl-3-(3-dimethy-laminopropyl) carbodiimide/N-hydroxysuccinimide (EDC/NHS, figure 3(m)) method [97]. These approaches enable the immobilization of biomolecules like antibodies, aptamers, or proteins onto the sensor surface for specific target binding. Before this surface functionalization step, MR sensors are typically surface coated with an ultrathin passivation layer made of materials such as SiO_2 and Si_3N_4. This layer serves a dual purpose: it protects the sensors from corrosion caused by exposure to biological samples and provides chemical sites for subsequent functionalization. However, the passivation layer thickness poses a critical design trade-off. It needs to be sufficiently thin to ensure the magnetic signals from the labels remain detectable by the sensor while being thick enough to prevent liquid leakage through any defects or pores. Typically, the passivation layer is on the order of tens of nanometers, balancing these competing requirements to maintain both the sensor's performance and durability in biological environments.

Finally, the integration of MR sensors into scalable and cost-effective biomedical devices presents additional challenges. Ensuring consistent performance across a large-scale production is crucial for widespread clinical adoption. This can be addressed by improving fabrication techniques such as using advanced lithography processes and automated quality control methods to ensure uniformity in sensor performance. Moreover, creating dense arrays of sensors in a compact format not only requires overcoming fabrication and

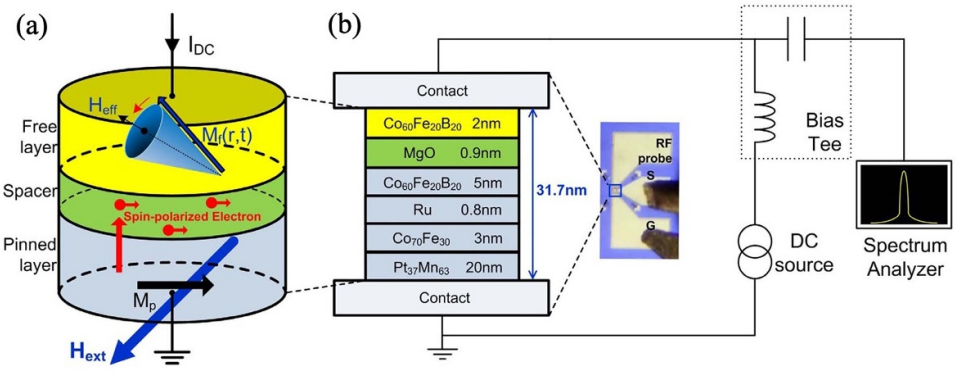

Figure 4. Schematics of (a) one STO device and (b) the setup for STO signal recording. Reproduced with permission from [100]. CC BY-NC-ND 4.0.

packaging complexities but also demands addressing high power consumption per unit area, which becomes a significant concern as array density increases. Possible solutions include optimizing sensor design to minimize energy usage, incorporating low-power circuitry, and employing advanced thermal management systems to dissipate heat efficiently [62, 98, 99].

4.2. STO and SHO

STO (other name: STNO, spin torque nano-oscillator) generates microwave-frequency signals by utilizing the STT effect in magnetic multilayer structures. It typically consists of either an MTJ or a GMR structure, which includes two major ferromagnetic layers: a pinned layer with a fixed magnetization direction and a free layer with a magnetization that can dynamically respond to external stimuli (see figure 4(a)). When a charge current flows perpendicularly through the structure, the pinned layer polarizes the electron spins, creating a spin-polarized current. As this spin-polarized current passes through the free layer, it transfers angular momentum, exerting a torque on the free layer's magnetization. This torque induces steady-state precession of the free layer's magnetization around an equilibrium axis, producing an oscillating magnetic state that generates microwave-frequency signals. This precession of the free layer's magnetization can be recorded as a resistance or voltage signal of the STO device. Figure 4(b) illustrates a typical structure of an STO device reported by Choi *et al* [100], and the corresponding circuitry used to measure its oscillatory behavior. In this setup, a DC is applied through the inductive branch of the circuit, while the resulting voltage oscillations generated by the STO are captured via RF microprobes connected to the capacitive branch of a bias tee. These oscillations are then analyzed using a spectrum analyzer, which records the output spectrum of the STO for further evaluation.

The frequency of precession is affected by the current, external magnetic field, and material properties, making STOs versatile for applications such as microwave generation, RF communication, and neuromorphic computing. Their nanoscale size and low power consumption make them attractive for high-frequency, energy-efficient signal processing. The first patent that proposed STO as a magnetic sensor was filed by Hitachi Global Storage Technologies Netherlands BV in 2009 [101]. The same team presented the concept of using an STO to detect magnetic fields by measuring the oscillation frequency of the device [102]. The authors experimentally observed a 2.55 GHz oscillation frequency shift with a linewidth of 220 MHz as the external magnetic field varied from −522 to −814 Oe. Several micromagnetic simulation studies have demonstrated the feasibility of using STO sensors to detect magnetic tags for

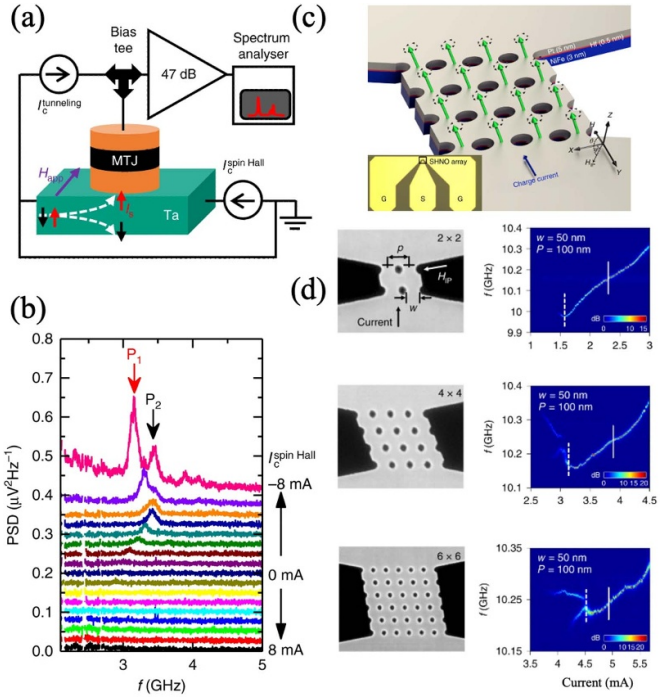

Figure 5. (a) Schematic of the microwave emission measurement circuit setup for SHO device. (b) Oscillation peak as a function of current. Reproduced from [105]. CC BY 4.0. (c) Schematic of a 4 × 4 SHNO array. The direction of the applied magnetic field H, its in-plane component H_{IP}, and the charge current are marked. The green arrows indicate the precessing magnetization of each SHNO. (d) Power spectral density of different SHNO arrays as a function of total drive current through the array. Scale bars are shown in dB over the noise floor. All data was acquired in a magnetic field of 0.68 T with an out-of-plane angle of 76° and an in-plane angle of 30°. Reproduced from [106], with permission from Springer Nature.

label-based biosensing [103, 104]. These studies highlight the theoretical capability of STO to achieve the detection limit of a single magnetic nanoparticle—single molecule detection.

Like STO, a SHO (other name: SHNO, spin Hall nano-oscillator) can also generate microwave-frequency signals by utilizing the SHE to convert charge currents into spin currents. As shown in figure 5(a), it typically consists of a heavy metal layer (e.g. Pt or Ta) with strong SOC. When an electric current flows through the heavy metal layer, the SHE generates a spin current perpendicular to the charge current direction. This spin current exerts SOT on the magnetization of the ferromagnetic layer, causing it to precess at high frequencies. The precessing magnetization emits electromagnetic waves in the microwave range, which can be tuned by adjusting the input current (see figure 5(b)) or an applied magnetic field. SHOs have been reported for applications in wireless communication, microwave signal generation, and neuromorphic computing as well.

Here, we categorize STOs and SHOs in the same sub-section due to their similar working principles for magnetic field sensing and label-based biosensing. In both devices, the magnetic field and magnetized magnetic tags influence the frequency of precession in the magnetization of the ferromagnetic layer. The frequency shift of these oscillators can be measured either through an MR device or by detecting microwave emissions, allowing them to function as highly sensitive magnetic quantum sensors.

For improved sensitivity of STO and SHO, an array of synchronized oscillators is suggested over a single oscillator to increase the operating frequency range and the microwave emission power output and, thus, enhance the SNR. Figure 5(c) shows the schematic of a 4 × 4 SHNO array. As shown in figure 5(d), by

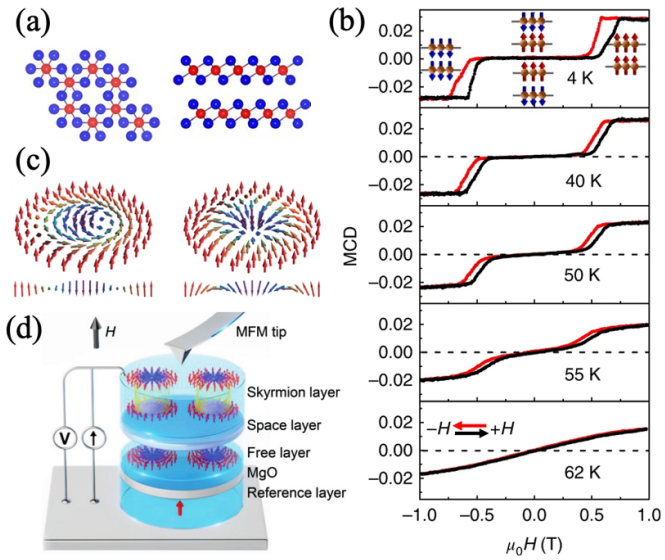

Figure 6. (a) Top view of monolayer CrI_3, where Cr atoms (red balls) form a honeycomb structure in an edge-sharing octahedral coordination by six I atoms (blue balls), and side view of bilayer CrI_3 of the rhombohedral stacking order. (b) Magnetic circular dichroism (MCD) signal as a function of applied magnetic field at different temperatures. Black and red lines show the forward and backward sweeps of the field, respectively. Insets (top) depict the magnetic states of bilayer CrI_3 under different magnetic fields. Reproduced from [108], with permission from Springer Nature. (c) Bloch (left) and Néel (right) type skyrmions. Arrows represent spins. The cross-section of the vortex is also depicted in both cases. Reproduced from [120], with permission from Springer Nature. (d) Schematic of the detection of skyrmions in an MTJ. Reproduced from [121]. CC BY 4.0.

increasing the number of oscillators that are synchronized, the SNR is enhanced. In addition, for reported STO and SHO, the oscillation peak linewidth typically ranges from a few MHz to hundreds of MHz. For high-performance magnetic sensors, achieving line widths in the kHz range or lower is desirable to detect ultra-low magnetic fields, particularly in applications like medical imaging applications. In addition to the specific challenges faced by oscillators, they share similar obstacles to MR sensors, as discussed in section 4.1.4, when being adapted for biomedical applications.

4.3. 2D vdW Magnets

2D vdW magnets are materials that exhibit magnetic properties in their monolayer or few-layer forms, with layers held together by weak vdW forces. These materials, such as CrI_3, retain their intrinsic magnetism even down to the monolayer limit [107]. The weak interlayer coupling as well as the magnetic properties of 2D vdW magnets are affected by electric and magnetic fields [108–110], pressure [111, 112], layer stacking [113, 114], and deposition of thin films on surfaces [115]. 2D vdW magnets hold promise in applications such as quantum computing and magnetic sensing.

The development of 2D vdW magnets for sensor applications is still in its early stages. Several groups have investigated the magnetization behavior of bilayer CrI_3 (figure 6(a)) under an out-of-plane (OOP) magnetic field [108, 116–119]. As shown in figure 6(b), at low temperatures, the bilayer exhibits an antiferromagnetic phase, with a spin-flip transition into a ferromagnetic phase observed at a moderate critical field of ∼0.6 T. This transition is attributed to the relatively weak interlayer exchange interaction. As the temperature increases, the spin-flip transition broadens. At 60 K, the magnetization (proportional to the measured MCD value) changes linearly as a function of the applied magnetic field [116], indicating that the bilayer CrI_3 becomes paramagnetic.

Although there is a long list of 2D vdW magnets reported, their unique magnetoelectric properties are mainly limited to $<$100 K temperature conditions. The room temperature ferromagnetic properties of VSe_2 and $MnSe_2$ monolayers may enable applications at ambient temperature, which is critical for biomedical applications without cryogenic conditions. An example of hybrid 2D vdW magnets designed for room temperature magnetic sensing is reported by Jimenez *et al* [122] The sensor operates based on changes in the resonance frequency of an LC circuit, which consists of a soft ferromagnetic microwire coil (approximately 60 μm in diameter, wound into a 15-turn, 10 mm long coil with a 5 mm internal diameter). The core of the coil is a monolayer VSe_2. The sensor achieves a sensitivity of 16 MHz Oe^{-1} (or 160 GHz T^{-1}), making it a promising candidate for a wide range of magnetic sensing applications.

The history of 2D vdW magnets is relatively recent, with significant breakthroughs over the past two decades as part of the broader exploration of 2D materials following graphene's isolation in 2004. A major milestone came in 2017 with the discovery of intrinsic magnetism in monolayer CrI_3 and bilayer $Cr_2Ge_2Te_6$, demonstrating how interlayer coupling and magnetic anisotropy stabilize long range magnetic order at low temperatures. Since then, new 2D vdW magnets have emerged, offering higher Curie temperatures and diverse magnetic properties, with reports of Fe_3GeTe_2 and Fe_3GaTe_2 achieving Curie temperatures at or above room temperature [123, 124]. Research now aims to improve thermal stability and expand applications at ambient temperatures. While still at its infant stage, the magnetic transitions of 2D vdW magnets under external magnetic fields show potential applications for ultra-low magnetic field sensing, which is of great interest for bio-magnetic field measurements.

At the research stage, various techniques are employed to measure the magnetization in 2D vdW magnets, including SQUID, magnetic force microscopy (MFM), x-ray magnetic circular dichroism (XMCD), spin-polarized scanning tunneling microscopy (SP-STM), ferromagnetic resonance (FMR), electron spin resonance (ESR), neutron scattering, and magneto-optical Kerr effect (MOKE) or magnetic circular dichroism (MCD) spectroscopy. These methods provide valuable insights into the magnetization of 2D vdW materials under varying magnetic fields and across different length scales. However, these bulky and expensive techniques are not ideal for biomedical applications, sharing similar limitations to SQUID and MRI.

To further enable the use of 2D vdW materials in practical biomedical applications, we give several approaches here. For instance, functionalizing the surface of 2D vdW magnets with biorecognition elements like antibodies, peptides, or DNA aptamers can allow for the selective detection of specific biomarkers in magnetic biosensing applications. These functionalized materials can act as active layers in sensors, binding target molecules to induce detectable changes in their magnetic properties. Additionally, combining 2D vdW magnets with flexible, biocompatible substrates can facilitate their integration into wearable or implantable devices for real-time, *in vivo* monitoring of bio-magnetic fields. Furthermore, the development of miniaturized, cost-effective readout systems, such as those employing compact MR devices or NV centers in diamonds, can overcome the limitations of bulky and expensive characterization techniques. These advancements, coupled with progress in scalable synthesis and transfer methods, will pave the way for the widespread adoption of 2D vdW magnets in high-sensitivity, next-generation biomedical diagnostics and imaging technologies.

4.4. Skyrmions

A skyrmion is a topologically stable, swirling configuration of spins in a magnetic material. The spins in a skyrmion point in different directions (see figure 6(c)).

Skyrmions are typically stabilized by the DMI in materials with strong SOC and broken inversion symmetry, and they can exist in ferromagnetic or antiferromagnetic systems. These structures are often just a few nanometers in size and can be moved with minimal electric current and magnetic fields. For example, Zhang *et al* reported that chiral skyrmions in Cu_2OSeO_3 can be effectively manipulated by a magnetic field gradient [125]. In a recent study, Koraltan *et al* experimentally demonstrated a skyrmion-based device using $[W/CoFeB/MgO]_{10}$ multilayers for three-dimensional magnetic field sensing at room temperature [126]. The skyrmion Hall bar device was used to measure both in-plane (IP) and OOP magnetic fields, with electrical readout based on the anomalous Hall effect. The device achieved a measurable linear range of ± 17 mT for IP fields and ± 30 mT for OOP fields. However, a significant challenge remains: the device experiences considerable temperature increases due to Joule heating. Although the sensitivity of this skyrmion device is currently orders of magnitude lower than that of commercial MTJ sensors, the authors proposed several strategies to enhance its sensitivity, offering the potential for future improvements.

With their high stability at room temperature, nanoscale size, and controllability, skyrmions are promising for applications such as high-density magnetic storage, racetrack memory, and neuromorphic computing. However, their potential for magnetic field sensing and imaging remains underexplored. One key challenge is that while skyrmions are stable at room temperature, subtle temperature variations can significantly influence their behavior. This poses a particular challenge for magnetic sensing and imaging applications, especially when interfacing with biological systems, where precise temperature control and stability are crucial. Material optimization, including the development of skyrmion-hosting heterostructures with enhanced thermal robustness and magnetic anisotropy, can further stabilize skyrmions at room temperature and reduce sensitivity to temperature fluctuations. Additionally, hybrid designs combining skyrmions with MR sensors (figure 6(d)) can leverage the sensitivity of MR technologies while enhancing the readout mechanisms, thus, significantly boosting the sensitivity of skyrmion-based sensors to weak bio-magnetic fields. Furthermore, encapsulating these devices in biocompatible materials, such as polyimide or parylene C, can ensure their safe integration into biological environments, enabling both wearable and implantable applications.

5. Conclusions and outlook

In the field of magnetic imaging and biosensing, magnetic sensors span a wide range from classical devices, such as Hall sensors, fluxgate sensors, and inductive sensors, to advanced quantum sensors like MR sensors and SQUIDs. In response to the growing interest in quantum sensors for biomedical applications, this perspective examines magnetic quantum sensors across commercial and lab stages. Our discussion begins by reviewing popular quantum sensors for magnetic imaging and sensing, including SQUID, MRI, OPM, NV magnetometers, and QDs. Among these, SQUID and MRI are already in clinical use for medical imaging and sensing. However, their reliance on cryogenic conditions results in high operational costs, limiting widespread adoption. In contrast, OPM, NV magnetometers, and QDs, which operate at ambient temperatures and have lower costs, hold significant potential to revolutionize biomedical applications as they advance beyond the lab stage.

Additionally, this perspective highlights emerging spintronic devices as next-generation magnetic quantum sensors for medical imaging and sensing. Table 2 summarizes the magnetic field detectivity of spintronic sensors and reported applications to date. Mature MR sensors, such as GMR and MTJ

Table 2. Summary of spintronic devices and reported applications.

Spintronic devices	Sensitivity	Cryogenic	Reported applications	Technological readiness level (TRL)
AMR	μT/sqrt(Hz)	No	Biosensors (Commercial)	Full scale product in commercial conditions
GMR	nT/sqrt(Hz)	No	Label-based biosensor (Commercial) Magnetic imaging (Conceptual)	Full scale product in commercial conditions
MTJ	pT/sqrt(Hz)	No	Label-based biosensor (Lab stage) Magnetic imaging (Conceptual)	Partial scale prototype validation
STO, SHO	$\sim$100s GHz T^{-1}	No	Magnetic sensing (Lab stage)	Partial scale prototype and modeling
2D vdW magnets	—	Yes	Magnetic sensing (Lab stage)	Technology conceptualized
Hybrid 2D vdW magnets designed as LC circuits	$\sim$100s GHz T^{-1}	No	Magnetic sensing (Lab stage)	Technology conceptualized
Skyrmions	—	No	Magnetic sensing (Lab stage)	Technology conceptualized & proof of concept validation

sensors, have already been commercialized and applied in magnetic biosensing. Preliminary lab-based studies on bio-magnetic field measurements using these sensors have demonstrated their potential for applications in magnetic imaging techniques such as MCG, MEG, and MMG. We also highlighted examples of emerging spintronic devices for magnetic sensing, including STOs, SHOs, 2D vdW magnets, and skyrmions. These technologies are currently at the lab-based stage and face challenges such as limited operational temperature ranges, susceptibility to environmental variations, lack of compact measurement techniques, and insufficient sensitivity. These technical hurdles reflect the relatively early stage of research in this field.

For nano- and micro-scale spintronic devices designed to interface with biological entities, such as biofluidic samples and biological tissues, several challenges must be addressed. These include the potential cytotoxicity of spintronic materials to biological systems, corrosion of devices due to environmental exposure or interfacing with biofluids, random noise affecting device performance, and the power consumption associated with high-density spintronic device arrays. These issues are already being actively studied and tackled, with ongoing advancements aimed at improving the compatibility, stability, and efficiency of spintronic devices in biomedical applications. With these, the authors believe that with another one to two decades of development, these emerging spintronic quantum sensors could be adapted for biomedical applications, enabling breakthroughs in single-molecule or single-cell detection, sub-micrometer resolution medical imaging, and protein structure analysis.

Data availability statement

No new data were created or analysed in this study.

Acknowledgment

This study was financially supported by Texas Tech University through HEF New Faculty Startup, NRUF Start Up, and Core Research Support Fund.

Author contributions

K W wrote Abstract, sections 1–3, 4.1, 4.2, and 5. R H wrote sections 4.3 and 4.4. Both authors proofread the manuscript.

ORCID iDs

Kai Wu https://orcid.org/0000-0002-9444-6112
Rui He https://orcid.org/0000-0002-2368-7269

References

[1] Anon Notice of special interest (NOSI): quantum sensing technologies in biomedical applications
[2] Aslam N, Zhou H, Urbach E K, Turner M J, Walsworth R L, Lukin M D and Park H 2023 Quantum sensors for biomedical applications *Nat. Rev. Phys.* **5** 157–69
[3] Shimazoe K, Tomita H, Watts D, Moskal P, Kagawa A, Thirolf P G, Budker D and Levin C S 2021 *Quantum Sensing for Biomedical Applications 2021 IEEE Nuclear Science Symp. and Medical Imaging Conf. (NSS/MIC)* (IEEE) pp 1–4
[4] Wu K *et al* 2024 Roadmap on magnetic nanoparticles in nanomedicine *Nanotechnology* **36** 042003
[5] Zhao B, Li L, Zhang Y, Tang J, Liu Y and Zhai Y 2023 Optically pumped magnetometers recent advances and applications in biomagnetism: a review *IEEE Sens. J.* **23** 18949–62
[6] Cheng H *et al* 2024 Wireless optically pumped magnetometer MEG *NeuroImage* **300** 120864
[7] Mostufa S, Yari P, Rezaei B, Xu K and Wu K 2023 Flexible magnetic field nanosensors for wearable electronics: a review *ACS Appl. Nano Mater.* **6** 13732–65
[8] Yang H, Li S, Wu Y, Bao X, Xiang Z, Xie Y, Pan L, Chen J, Liu Y and Li R 2024 Advances in flexible magnetosensitive materials and devices for wearable electronics *Adv. Mater.* **36** 2311996
[9] Ashammakhi N *et al* 2021 Biodegradable implantable sensors: materials design, fabrication, and applications *Adv. Funct. Mater.* **31** 2104149
[10] Zuo S, Heidari H, Farina D and Nazarpour K 2020 Miniaturized magnetic sensors for implantable magnetomyography *Adv. Mater. Technol.* **5** 2000185
[11] Wu K, Su D, Saha R and Wang J-P 2022 Giant magnetoresistance (GMR) materials and devices for biomedical and industrial applications *Spintron. Mater. Devices Appl.* ed K Wang, M Yang and J Luo pp 3–49
[12] Wu K, Tonini D, Liang S, Saha R, Chugh V K and Wang J-P 2022 Giant magnetoresistance biosensors in biomedical applications *ACS Appl. Mater. Interfaces* **14** 9945–69
[13] Sochnikov I, Davino D and Kalisky B 2020 dc SQUID design with femtotesla sensitivity for quantum-ready readouts *Phys. Rev. Appl.* **14** 014020
[14] Rudd J, Chubak G, Larnier H, Stolz R, Schiffler M, Zakosarenko V, Schneider M, Schulz M and Meyer M 2022 Commercial operation of a SQUID-based airborne magnetic gradiometer *Lead. Edge* **41** 486–92
[15] Storm J-H, Hömmen P, Drung D and Körber R 2017 An ultra-sensitive and wideband magnetometer based on a superconducting quantum interference device *Appl. Phys. Lett.* **110** 072603
[16] Zotev V S, Matlachov A N, Volegov P L, Sandin H J, Espy M A, Mosher J C, Urbaitis A V, Newman S G and Kraus R H 2007 Multi-channel SQUID system for MEG and ultra-low-field MRI *IEEE Trans. Appl. Supercond.* **17** 839–42
[17] Zhang Y, Qin X, Liu G, Wang C, Li Q, Yuan J and Liu W 2024 Enhancing precision in SQUID sensors: analyzing washer geometry dependence at the microscale *Appl. Sci.* **14** 6212
[18] Brookes M J, Leggett J, Rea M, Hill R M, Holmes N, Boto E and Bowtell R 2022 Magnetoencephalography with optically pumped magnetometers (OPM-MEG): the next generation of functional neuroimaging *Trends Neurosci.* **45** 621–34
[19] Hill R M *et al* 2020 Multi-channel whole-head OPM-MEG: helmet design and a comparison with a conventional system *NeuroImage* **219** 116995
[20] Clarke J and Koch R H 1988 The impact of high-temperature superconductivity on SQUID magnetometers *Science* **242** 217–23

[21] Vlaardingerbroek M T and Boer J A 2013 *Magnetic Resonance Imaging: Theory and Practice* (Springer Science & Business Media)
[22] Lohrke J *et al* 2016 25 years of contrast-enhanced MRI: developments, current challenges and future perspectives *Adv. Ther.* **33** 1–28
[23] Serai S D 2022 Basics of magnetic resonance imaging and quantitative parameters T1, T2, T2*, T1rho and diffusion-weighted imaging *Pediatr. Radiol.* **52** 217–27
[24] Manso Jimeno M, Vaughan J T and Geethanath S 2023 Superconducting magnet designs and MRI accessibility: a review *NMR Biomed.* **36** e4921
[25] Tadic T and Fallone B G 2012 Design and optimization of superconducting MRI magnet systems with magnetic materials *IEEE Trans. Appl. Supercond.* **22** 4400107
[26] Wachowicz K 2014 Evaluation of active and passive shimming in magnetic resonance imaging *Res. Rep. Nucl. Med.* **4** 1–12
[27] Kong X, Zhu M, Xia L, Crozier S, Wang Q, Ni Z and Liu F 2015 A novel passive shimming method for the correction of magnetic fields above the patient bed in MRI *J. Magn. Reson.* **257** 64–69
[28] Oelsner G, IJsselsteijn R, Scholtes T, Krüger A, Schultze V, Seyffert G, Werner G, Jäger M, Chwala A and Stolz R 2022 Integrated optically pumped magnetometer for measurements within Earth's magnetic field *Phys. Rev. Appl.* **17** 024034
[29] Zhang S, Lu J, Ye M, Zhou Y, Yin K, Lu F, Yan Y and Zhai Y 2022 Optimal operating temperature of miniaturized optically pumped magnetometers *IEEE Trans. Instrum. Meas.* **71** 1–7
[30] Savukov I, Kim Y J, Shah V and Boshier M G 2017 High-sensitivity operation of single-beam optically pumped magnetometer in a kHz frequency range *Meas. Sci. Technol.* **28** 035104
[31] Alem O, Mhaskar R, Jiménez-Martínez R, Sheng D, LeBlanc J, Trahms L, Sander T, Kitching J and Knappe S 2017 Magnetic field imaging with microfabricated optically-pumped magnetometers *Opt. Express* **25** 7849
[32] Boto E *et al* 2018 Moving magnetoencephalography towards real-world applications with a wearable system *Nature* **555** 657–61
[33] Feys O, Corvilain P, Aeby A, Sculier C, Holmes N, Brookes M, Goldman S, Wens V and De Tiège X 2022 On-scalp optically pumped magnetometers versus cryogenic magnetoencephalography for diagnostic evaluation of epilepsy in school-aged children *Radiology* **304** 429–34
[34] Wittevrongel B, Holmes N, Boto E, Hill R, Rea M, Libert A, Khachatryan E, Van Hulle M M, Bowtell R and Brookes M J 2021 Practical real-time MEG-based neural interfacing with optically pumped magnetometers *BMC Biol.* **19** 158
[35] Jodko-Władzińska A, Wildner K, Pałko T and Władziński M 2020 Compensation system for biomagnetic measurements with optically pumped magnetometers inside a magnetically shielded room *Sensors* **20** 4563
[36] Nordenström S, Lebedev V, Hartwig S, Kruse M, Marquetand J, Broser P and Middelmann T 2024 Feasibility of magnetomyography with optically pumped magnetometers in a mobile magnetic shield *Sci. Rep.* **14** 18960
[37] Mardell L C, Spedden M E, O'Neill G C, Tierney T M, Timms R C, Zich C, Barnes G R and Bestmann S 2024 Concurrent spinal and brain imaging with optically pumped magnetometers *J. Neurosci. Methods* **406** 110131
[38] Stürner F M *et al* 2021 Integrated and portable magnetometer based on nitrogen-vacancy ensembles in diamond *Adv. Quantum Technol.* **4** 2000111
[39] Acosta V M, Bouchard L S, Budker D, Folman R, Lenz T, Maletinsky P, Rohner D, Schlussel Y and Thiel L 2019 Color centers in diamond as novel probes of superconductivity *J. Supercond. Nov. Magn.* **32** 85–95
[40] Zhang C *et al* 2021 Diamond magnetometry and gradiometry towards subpicotesla dc field measurement *Phys. Rev. Appl.* **15** 064075
[41] Wang X *et al* 2022 Portable diamond NV magnetometer head integrated with 520 nm diode laser *IEEE Sens. J.* **22** 5580–7
[42] Dolde F *et al* 2011 Electric-field sensing using single diamond spins *Nat. Phys.* **7** 459–63
[43] Michl J *et al* 2019 Robust and accurate electric field sensing with solid state spin ensembles *Nano Lett.* **19** 4904–10
[44] Neumann P *et al* 2013 High-precision nanoscale temperature sensing using single defects in diamond *Nano Lett.* **13** 2738–42
[45] Choe S, Yoon J, Lee M, Oh J, Lee D, Kang H, Lee C-H and Lee D 2018 Precise temperature sensing with nanoscale thermal sensors based on diamond NV centers *Curr. Appl. Phys.* **18** 1066–70
[46] Mzyk A, Ong Y, Ortiz Moreno A R, Padamati S K, Zhang Y, Reyes-San-Martin C A and Schirhagl R 2022 Diamond color centers in diamonds for chemical and biochemical analysis and visualization *Anal. Chem.* **94** 225–49
[47] Zhang T *et al* 2021 Toward quantitative bio-sensing with nitrogen–vacancy center in diamond *ACS Sens.* **6** 2077–107
[48] Khazen K and Von Bardeleben H J 2023 NV-centers in SiC: a solution for quantum computing technology? *Front. Quantum Sci. Technol.* **2** 1115039

[49] Prawer S and Greentree A D 2008 Diamond for quantum computing *Science* **320** 1601–2
[50] Tsukamoto M, Ogawa K, Ozawa H, Iwasaki T, Hatano M, Sasaki K and Kobayashi K 2021 Vector magnetometry using perfectly aligned nitrogen-vacancy center ensemble in diamond *Appl. Phys. Lett.* **118** 264002
[51] Misonou D, Sasaki K, Ishizu S, Monnai Y, Itoh K M and Abe E 2020 Construction and operation of a tabletop system for nanoscale magnetometry with single nitrogen-vacancy centers in diamond *AIP Adv.* **10** 025206
[52] Tufani A, Qureshi A and Niazi J H 2021 Iron oxide nanoparticles based magnetic luminescent quantum dots (MQDs) synthesis and biomedical/biological applications: a review *Mater. Sci. Eng.* C **118** 111545
[53] Yamada S, Yukawa H, Yamada K, Murata Y, Jo J, Yamamoto M, Sugawara-Narutaki A, Tabata Y and Baba Y 2022 *In vivo* multimodal imaging of stem cells using nanohybrid particles incorporating quantum dots and magnetic nanoparticles *Sensors* **22** 5705
[54] Chern M, Kays J C, Bhuckory S and Dennis A M 2019 Sensing with photoluminescent semiconductor quantum dots *Methods Appl. Fluoresc.* **7** 012005
[55] Ge Z, Slizovskiy S, Polizogopoulos P, Joshi T, Taniguchi T, Watanabe K, Lederman D, Fal'ko V I and Velasco J 2023 Giant orbital magnetic moments and paramagnetic shift in artificial relativistic atoms and molecules *Nat. Nanotechnol.* **18** 250–6
[56] Chinnathambi S, Chen S, Ganesan S and Hanagata N 2014 Silicon quantum dots for biological applications *Adv. Healthcare Mater.* **3** 10–29
[57] Tong L, Qiu F, Zeng T, Long J, Yang J, Wang R, Zhang J, Wang C, Sun T and Yang Y 2017 Recent progress in the preparation and application of quantum dots/graphene composite materials *RSC Adv.* **7** 47999–8018
[58] Rezaei B *et al* 2024 Effect of polymer and cell membrane coatings on theranostic applications of nanoparticles: a review *Adv. Healthcare Mater.* **13** 2401213
[59] Julliere M 1975 Tunneling between ferromagnetic films *Phys. Lett.* A **54** 225–6
[60] Baibich M N, Broto J M, Fert A, Van Dau F N, Petroff F, Etienne P, Creuzet G, Friederich A and Chazelas J 1988 Giant magnetoresistance of (001) Fe/(001) Cr magnetic superlattices *Phys. Rev. Lett.* **61** 2472
[61] Binasch G, Grünberg P, Saurenbach F and Zinn W 1989 Enhanced magnetoresistance in layered magnetic structures with antiferromagnetic interlayer exchange *Phys. Rev.* B **39** 4828–30
[62] Guo Z, Yin J, Bai Y, Zhu D, Shi K, Wang G, Cao K and Zhao W 2021 Spintronics for energy-efficient computing: an overview and outlook *Proc. IEEE* **109** 1398–417
[63] Puebla J, Kim J, Kondou K and Otani Y 2020 Spintronic devices for energy-efficient data storage and energy harvesting *Commun. Mater.* **1** 24
[64] Mostufa S, Liang S, Chugh V K, Wang J-P and Wu K 2024 Spintronic devices for biomedical applications *npj Spintron.* **2** 26
[65] Ritzinger P and Výborný K 2023 Anisotropic magnetoresistance: materials, models and applications *R. Soc. Open Sci.* **10** 230564
[66] Wu K, Klein T, Krishna V D, Su D, Perez A M and Wang J-P 2017 Portable GMR handheld platform for the detection of influenza A virus *ACS Sens.* **2** 1594–601
[67] Choi J, Gani A W, Bechstein D J, Lee J-R, Utz P J and Wang S X 2016 Portable, one-step, and rapid GMR biosensor platform with smartphone interface *Biosens. Bioelectron.* **85** 1–7
[68] Udomsom S, Mankong U, Paengnakorn P and Theera-Umpon N 2021 Novel rapid protein coating technique for silicon photonic biosensor to improve surface morphology and increase bioreceptor density *Coatings* **11** 595
[69] Guedes A, Macedo R, Jaramillo G, Cardoso S, Freitas P P and Horsley D A 2018 Hybrid GMR sensor detecting 950 pT/sqrt (Hz) at 1 Hz and room temperature *Sensors* **18** 790
[70] Baselt D R, Lee G U, Natesan M, Metzger S W, Sheehan P E and Colton R J 1998 A biosensor based on magnetoresistance technology *Biosens. Bioelectron.* **13** 731–9
[71] Bayin Q, Huang L, Ren C, Fu Y, Ma X and Guo J 2021 Anti-SARS-CoV-2 IgG and IgM detection with a GMR based LFIA system *Talanta* **227** 122207
[72] Krishna V D, Wu K, Perez A M and Wang J P 2016 Giant magnetoresistance-based biosensor for detection of influenza A virus *Front. Microbiol.* **7** 8
[73] Su D, Wu K, Krishna V, Klein T, Liu J, Feng Y, Perez A M, Cheeran M C and Wang J-P 2019 Detection of influenza a virus in swine nasal swab samples with a wash-free magnetic bioassay and a handheld giant magnetoresistance sensing system *Front. Microbiol.* **10** 1077
[74] Ng E, Le A K, Nguyen M H and Wang S X 2020 Early multiplexed detection of cirrhosis using giant magnetoresistive biosensors with protein biomarkers *ACS Sens.* **5** 3049–57
[75] Gani A W, Wei W, Shi R-Z, Ng E, Nguyen M, Chua M-S, So S and Wang S X 2019 An automated, quantitative, and multiplexed assay suitable for point-of-care hepatitis B virus diagnostics *Sci. Rep.* **9** 1–11
[76] Zhi X, Liu Q S, Zhang X, Zhang Y X, Feng J and Cui D X 2012 Quick genotyping detection of HBV by giant magnetoresistive biochip combined with PCR and line probe assay *Lab Chip* **12** 741–5

[77] Zhi X, Deng M, Yang H, Gao G, Wang K, Fu H, Zhang Y, Chen D and Cui D 2014 A novel HBV genotypes detecting system combined with microfluidic chip, loop-mediated isothermal amplification and GMR sensors *Biosens. Bioelectron.* **54** 372–7

[78] Klein T, Wang W, Yu L, Wu K, Boylan K L, Vogel R I, Skubitz A P and Wang J-P 2019 Development of a multiplexed giant magnetoresistive biosensor array prototype to quantify ovarian cancer biomarkers *Biosens. Bioelectron.* **126** 301–7

[79] Xu L, Yu H, Akhras M S, Han S-J, Osterfeld S, White R L, Pourmand N and Wang S X 2008 Giant magnetoresistive biochip for DNA detection and HPV genotyping *Biosens. Bioelectron.* **24** 99–103

[80] Ravi N, Rizzi G, Chang S E, Cheung P, Utz P J and Wang S X 2019 Quantification of cDNA on GMR biosensor array towards point-of-care gene expression analysis *Biosens. Bioelectron.* **130** 338–43

[81] Rizzi G, Lee J R, Dahl C, Guldberg P, Dufva M, Wang S X and Hansen M F 2017 Simultaneous profiling of DNA mutation and methylation by melting analysis using magnetoresistive biosensor array *ACS Nano* **11** 8864–70

[82] Amaral J, Cardoso S, Freitas P and Sebastião A 2011 Toward a system to measure action potential on mice brain slices with local magnetoresistive probes *J. Appl. Phys.* **109** 07B308

[83] Caruso L *et al* 2017 *In vivo* magnetic recording of neuronal activity *Neuron* **95** 1283–91

[84] Oogane M *et al* 2021 Sub-pT magnetic field detection by tunnel magneto-resistive sensors *Appl. Phys. Express* **14** 123002

[85] Scheike T, Wen Z, Sukegawa H and Mitani S 2023 631% room temperature tunnel magnetoresistance with large oscillation effect in CoFe/MgO/CoFe(001) junctions *Appl. Phys. Lett.* **122** 112404

[86] Sharma P P *et al* 2017 Integrated platform for detecting pathogenic DNA via magnetic tunneling junction-based biosensors *Methods Appl. Fluoresc. Methods* **242** 280–7

[87] Sharma P P *et al* 2017 Towards a magnetoresistive platform for neural signal recording *AIP Adv.* **7** 056706

[88] Fujiwara K *et al* 2018 Magnetocardiography and magnetoencephalography measurements at room temperature using tunnel magneto-resistance sensors *Appl. Phys. Express* **11** 023001

[89] Wang M, Wang Y, Peng L and Ye C 2019 Measurement of triaxial magnetocardiography using high sensitivity tunnel magnetoresistance sensor *IEEE Sens. J.* **19** 9610–5

[90] Moretti D, DiFrancesco M L, Sharma P P, Dante S, Albisetti E, Monticelli M, Bertacco R, Petti D, Baldelli P and Benfenati F 2018 Biocompatibility of a magnetic tunnel junction sensor array for the detection of neuronal signals in culture *Front. Neurosci.* **12** 909

[91] Yang S and Zhang J 2021 Current progress of magnetoresistance sensors *Chemosensors* **9** 211

[92] Kim J, Park H, Jung D and Kim S 2003 Protein immobilization on plasma-polymerized ethylenediamine-coated glass slides *Anal. Biochem.* **313** 41–45

[93] Yin H B, Brown T, Wilkinson J S, Eason R W and Melvin T 2004 Submicron patterning of DNA oligonucleotides on silicon *Nucleic Acids Res.* **32** e118

[94] Shang X, Zhu Y and Li Z 2017 Surface modification of silicon carbide with silane coupling agent and hexadecyl iodiele *Appl. Surf. Sci.* **394** 169–77

[95] Saengdee P, Chaisriratanakul W, Bunjongpru W, Sripumkhai W, Srisuwan A, Jeamsaksiri W, Hruanun C, Poyai A and Promptmas C 2015 Surface modification of silicon dioxide, silicon nitride and titanium oxynitride for lactate dehydrogenase immobilization *Biosens. Bioelectron.* **67** 134–8

[96] Wang W, Wang Y, Tu L, Klein T, Feng Y L and Wang J P 2013 Surface modification for protein and DNA immobilization onto GMR biosensor *IEEE Trans. Magn.* **49** 296–9

[97] Mak A C, Osterfeld S J, Yu H, Wang S X, Davis R W, Jejelowo O A and Pourmand N 2010 Sensitive giant magnetoresistive-based immunoassay for multiplex mycotoxin detection *Biosens. Bioelectron.* **25** 1635–9

[98] He Z and Fan D 2017 Energy efficient reconfigurable threshold logic circuit with spintronic devices *IEEE Trans. Emerg. Top. Comput.* **5** 223–37

[99] Uchida K and Iguchi R 2021 Spintronic thermal management *J. Phys. Soc. Jpn.* **90** 122001

[100] Choi H S *et al* 2014 Spin nano–oscillator–based wireless communication *Sci. Rep.* **4** 5486

[101] Mesquita Braganca P, Gurney B A and Wilson B A Spin torque oscillator sensor

[102] Braganca P M, Gurney B A, Wilson B A, Katine J A, Maat S and Childress J R 2010 Nanoscale magnetic field detection using a spin torque oscillator *Nanotechnology* **21** 235202

[103] Xia H, Zheng Q, Mu C, Song C, Jin C, Liu Q and Wang J 2017 Micromagnetic simulation for detection of magnetic nanobeads by spin torque oscillator *J. Magn. Magn. Mater.* **432** 387–90

[104] Saha R, Wu K, Su D and Wang J-P 2020 Spin current nano-oscillator (SCNO) as a potential frequency-based, ultra-sensitive magnetic biosensor: a simulation study *Nanotechnology* **31** 375501

[105] Tarequzzaman M *et al* 2019 Spin torque nano-oscillator driven by combined spin injection from tunneling and spin Hall current *Commun. Phys.* **2** 20

[106] Zahedinejad M, Awad A A, Muralidhar S, Khymyn R, Fulara H, Mazraati H, Dvornik M and Åkerman J 2020 Two-dimensional mutually synchronized spin Hall nano-oscillator arrays for neuromorphic computing *Nat. Nanotechnol.* **15** 47–52
[107] Huang B *et al* 2017 Layer-dependent ferromagnetism in a van der Waals crystal down to the monolayer limit *Nature* **546** 270–3
[108] Jiang S, Shan J and Mak K F 2018 Electric-field switching of two-dimensional van der Waals magnets *Nat. Mater.* **17** 406–10
[109] Huang B *et al* 2018 Electrical control of 2D magnetism in bilayer CrI_3 *Nat. Nanotechnol.* **13** 544–8
[110] Li S *et al* 2020 Magnetic-field-induced quantum phase transitions in a van der Waals magnet *Phys. Rev.* X **10** 011075
[111] Li T *et al* 2019 Pressure-controlled interlayer magnetism in atomically thin CrI_3 *Nat. Mater.* **18** 1303–8
[112] Song T *et al* 2019 Switching 2D magnetic states via pressure tuning of layer stacking *Nat. Mater.* **18** 1298–302
[113] Guo X *et al* 2021 Structural monoclinicity and its coupling to layered magnetism in few-layer CrI_3 *ACS Nano* **15** 10444–50
[114] Xie H *et al* 2022 Twist engineering of the two-dimensional magnetism in double bilayer chromium triiodide homostructures *Nat. Phys.* **18** 30–36
[115] Nnokwe C *et al* 2025 Tuning the magnetic properties of CrI_3 using Ni thin film deposition for applications in spintronic devices *ACS Appl. Nano Mater.* **8** 2412–20
[116] Xie H *et al* 2023 Evidence of non-collinear spin texture in magnetic moiré superlattices *Nat. Phys.* **19** 1150–5
[117] Xu Y *et al* 2022 Coexisting ferromagnetic–antiferromagnetic state in twisted bilayer CrI_3 *Nat. Nanotechnol.* **17** 143–7
[118] Jin W *et al* 2020 Tunable layered-magnetism–assisted magneto-Raman effect in a two-dimensional magnet CrI_3 *Proc. Natl Acad. Sci.* **117** 24664–9
[119] Cenker J *et al* 2021 Direct observation of two-dimensional magnons in atomically thin CrI_3 *Nat. Phys.* **17** 20–25
[120] Kézsmárki I *et al* 2015 Néel-type skyrmion lattice with confined orientation in the polar magnetic semiconductor GaV4S8 *Nat. Mater.* **14** 1116–22
[121] Guang Y *et al* 2023 Electrical detection of magnetic skyrmions in a magnetic tunnel junction *Adv. Electron. Mater.* **9** 2200570
[122] Jimenez V O, Kalappattil V, Eggers T, Bonilla M, Kolekar S, Huy P T, Batzill M and Phan M-H 2020 A magnetic sensor using a 2D van der Waals ferromagnetic material *Sci. Rep.* **10** 4789
[123] Deng Y *et al* 2018 Gate-tunable room-temperature ferromagnetism in two-dimensional Fe_3GeTe_2 *Nature* **563** 94–99
[124] Zhang G, Guo F, Wu H, Wen X, Yang L, Jin W, Zhang W and Chang H 2022 Above-room-temperature strong intrinsic ferromagnetism in 2D van der Waals Fe_3GaTe_2 with large perpendicular magnetic anisotropy *Nat. Commun.* **13** 5067
[125] Zhang S L, Wang W W, Burn D M, Peng H, Berger H, Bauer A, Pfleiderer C, Van Der Laan G and Hesjedal T 2018 Manipulation of skyrmion motion by magnetic field gradients *Nat. Commun.* **9** 2115
[126] Koraltan S *et al* 2024 Skyrmionic device for three dimensional magnetic field sensing enabled by spin-orbit torques (arXiv:2403.16725)